SAND2001-1440
Unlimited Release
Printed May 2001

# BACKWARD INTEGRATION OF THE EQUATIONS OF MOTION TO CORRECT FOR FREE SURFACE PERTURBATIONS

Dennis Hayes
Shock Physics Applications
Sandia National Laboratories
P.O. Box 5800
Albuquerque, NM 87185-1181

## Abstract

Window and free surface interfaces perturb the flow in compression wave experiments. The velocity of these interfaces is routinely measured in shock-compression experiments using interferometry (i.e., VISAR). Interface perturbations often must be accounted for before meaningful material property results can be obtained. For shockless experiments when stress is a single valued function of strain, the governing equations of motion are hyperbolic and can be numerically integrated forward or backward in either time or space with assured stability. Using the VISAR results as "initial conditions" the flow fields are integrated backward in space to the interior of the specimen where the VISAR interface has not perturbed the flow at earlier times and results can be interpreted as if the interface had not been present. This provides a rather exact correction for free surface perturbations. The method can also be applied to window interfaces by selecting the appropriate initial conditions. Applications include interpreting Z-accelerator ramp wave experiments. The method applies to multiple layers and multiple reverberations.

For an elastic-plastic material model the flow is dissipative and the governing equations are parabolic. When the parabolic terms are small, the equations also can be successfully integrated backward in space. This is verified by using a traditional elastic-plastic wave propagation code with a backward-derived stress history as the boundary condition for a forward calculation. Calculated free surface histories match the starting VISAR record verifying that the backward method produced an accurate solution to the governing equations. With our cooperation, workers at Los Alamos have successfully applied the Sandia-developed backward technique for the time-dependent quasielastic material model and are analyzing stress histories at a spall plane using the VISAR free surface velocity measurement from a "pullback" experiment.

# Acknowledgements

This work has benefited from discussions with Clint Hall, Jim Asay and Marcus Knudsen from Sandia Labs and with Joe Fritz from Los Alamos National Lab.

# Table of Contents

# Figures

# Background and Summary

The backward integration technique was motivated by the need analyze experimental results from the Z-accelerator. These experiments measure free surface velocity for two or more specimen thicknesses using VISAR interferometry [1]. The desire is to interpret these signals by assuming the particle velocity characteristics are straight lines in space-time and thus infer the wave speed as a function of particle velocity. This is sufficient to determine the stress-strain behavior of the specimen material through Reimann invariants. The central problem is as follows: as early parts of the ramp wave arrive at the free surface, they reflect and interact with the later parts of the oncoming ramp wave. This interaction bends the oncoming characteristics negating the assumption of straight-line behavior required for conventional analysis techniques. Since ramp waves steepen with propagation distance, perturbations are different for each specimen thickness. In the case of the Z experiments this perturbation introduces unacceptably large errors in the desired result and the free surface interactions must be corrected for.

For example, Figure 1 shows calculated perturbations caused by free surface reflections for a typical ramp load on Z. The free surface perturbation is seen to be large for interface velocities above about 0.5km/s. If characteristics did not bend near the free surface, half

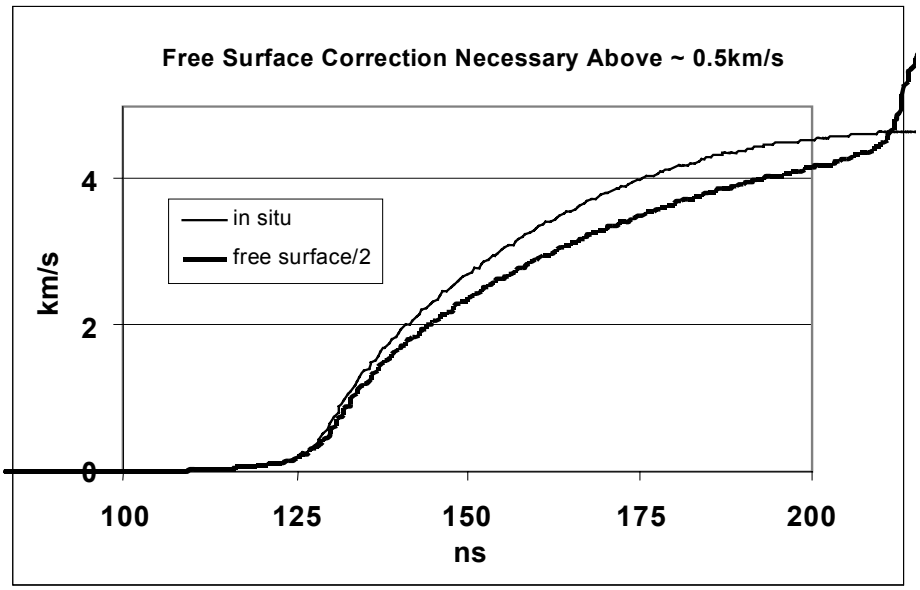


**Figure 1.** Example of perturbation caused by a free surface. To determine Lagrangian sound speed, experimenters make measurements of free surface velocity for two different thicknesses of specimen material. (Result for only one thickness is shown in this figure). Lagrangian sound speed at some particle velocity should be determined by dividing specimen thickness difference by arrival time difference of the *in situ* velocity. Errors are incurred if the *in situ* velocity is approximated by dividing the free surface result by two. The backward method is the most accurate way we have found for treating the data.

of the free surface velocity would exactly equal the *in situ* velocity. For an isentropic compression experiment on Z, two specimens of different thickness are subjected to identical loads and the free surface motion of each is monitored allowing the Lagrangian sound speed as a function of particle velocity amplitude to be obtained. This is done by dividing the difference in specimen thicknesses by the difference in the arrival times of a given *in situ* particle velocity amplitude for each specimen. There are two error considerations whenever the *in situ* velocity is estimated as one-half of the free surface velocity: one first order and the other second order. The first order error is easily seen in Figure 1; namely $u_{fs}(t)/2 < u_{is}(t)$ for all times and the difference increases with increasing velocity. This means that at the higher particle velocities, there is an increasingly large error in estimating the correct *in situ* particle velocity associated with a given amplitude of directly-measured free surface velocity. The more important error is second order. When the free surface records are directly analyzed using the above procedure, some of the free surface perturbation is common to each record and therefore "cancels" in the data reduction procedure. But since the ramp is steeper for the thicker sample, the correction is not the same for each record and there is a residual error in time difference not accounted for. This second error is not shown in figure 1 but is typically of the order of several nanoseconds, which is unacceptable given the accuracy requirements for the Z environment.

Various methods for addressing free surface or window perturbations have been used. One method compares calculations of the *in situ* particle velocity history for a specimen with another calculation with the free surface present [2]. Twice the calculated *in situ* velocity for the specimen is compared with the free surface velocity at the same Lagrangian position and a time or amplitude offset determined at each free surface particle velocity amplitude. This offset is determined for each specimen thickness and these offsets are then used to correct the times from the free surface measurements. The difficulty is that the correction depends upon the result, is non-unique and cannot differentiate between delay in arrival of the characteristic and the change in magnitude of the free surface motion associated with the given characteristic. Furthermore, the free surface velocity does not typically reach twice the *in situ* velocity meaning that the corrections vary from small at low velocity to big at large velocity, which makes accuracy difficult to quantify.

Another method (our earliest attempt) assumes a ramp wave steepens with distance in an orderly way and attempts to find time corrections from dimensional analysis. Although this showed some promise, it was too general and suffered from many of the same difficulties as the above approach.

Prior work [3] made approximate corrections by solving for the interactions near the free surface using an iterative Reimann invariant technique. This method was unacceptable for our problem.

The brute force forward calculation method supposes the load history is known and integrates forward in time using a traditional "hydrodynamic" code, varying the load and stress-strain relationship for the sample until experimental records are matched. This

method is typically difficult if not impossible to use when both the load history and the material properties are unknown and sometimes produces results that are not unique. For experiments where specimen properties are known and only the load history is to be determined, or *vice versa*, it is possible to find adequate solutions. The former is the case in some plate impact experiments and iterative procedures have been used to interpret free surface measurements. However, the process is cumbersome and this kind of problem is usually of low interest for experiments on Z.

The approach here is quite simple: use the equations of motion and a VISAR measurement to numerically integrate backwards in space, toward the loading surface, to a region that is interaction-free. In effect this is what Z experimenters had desired to do when they performed their experiments and used the previously described time corrections. The difference is that we numerically integrate using the equations of motion. It is worth noting that our method automatically corrects for the free surface or window perturbations and for a class of material types where stress is a single valued function of strain, this correction is essentially exact. And we have numerical evidence that the free surface corrections achieved by the backward method are also quite accurate for elastic-plastic and for quasielastic materials.

Although this method was developed for free surface corrections, it is easily applied to experiments in which the VISAR measurement surface of the specimen has an interferometer window. Rather than specify free surface history (free-surface particle velocity, zero stress, ambient density) as the "initial condition for the numerical integration, one need only specify the window history (window particle velocity, window stress, specimen density at that stress) as that "initial condition". This is easily done whenever the window has a known relationship between the first two quantities. Aside from providing the initial condition, the window plays no role in the subsequent integration. An example is shown in the body of this report.

It is also obvious that the backwards integration can be through multiple layers, or can be continued through multiple reverberations in some of those layers, provided care is taken not to violate the boundary condition at the loading surface.

The backward integration technique can be applied to single VISAR records whenever it is desired to infer the loading history. To do this, the stress-strain response of the specimen must be known.

If there are multiple VISAR records taken simultaneously on specimens of different thickness, it is possible to integrate each backward to the same interior position - say the original loading surface. Each record should produce the same result since the same load history was applied to each specimen. If these calculated loads do not agree, the assumed stress-strain behavior must be incorrect. We parameterize the stress-strain behavior (i.e., a two-parameter Murnaghan $B_O$, $B'$) or Lagrangian wave speed as a quartic polynomial in stress, etc. and systematically vary the parameters until the two (or more) inferred load histories agree. Thus analysis of two or more records is not only used to calculate the load history but also defines the stress-strain behavior of the specimens.

At Los Alamos National Laboratory (LANL), we have successfully integrated a free-surface record from a spall experiment back to the damage plane to infer the stress-strain history during failure. This entails introducing time-dependent, quasielastic strength behavior into the material model [4]. Although the equations for this case are parabolic and therefore may become unstable, a subsequent forward calculation using the backward-deduced stress history applied to a specimen of thickness equaling the scab thickness produces a calculated free surface motion that matches the measured result. This addition to the technique will be described in a forthcoming report [5].

At present, the method cannot be used if shocks are present anywhere in the flow. Since shocks produce entropy, which destroys information, there are simply regions of the x-t plane that are inaccessible by information obtained at the measurement surface. As a practical matter, if a shock is present in the VISAR record, it immediately begins to spread into an isentropic compression wave as the integration proceeds back into the interior of the specimen. Thus for large amplitude shocks, significant entropy generation will be ignored during backward integration. But for low amplitude shocks like the 20kbar shock present in the spall experiment, the entropy generated by the shock is completely negligible and apparently, as evidenced by the good comparison with the subsequent forward calculation, solutions are accurate enough for our purposes. Thus if we use the method for experiments with weak shocks, a case by case evaluation will be made to assess if errors introduced are significant.

We have not explored material behavior with irregular stress-strain behavior such as materials that undergo an equilibrium polymorphic phase change. Typically, phase changes have large volume changes and the shock process produces significant entropy meaning the parabolic terms in the governing equations are not necessarily small. It remains to be determined if such equations can be successfully integrated backward with manageable growth in the expected instabilities.

## Reducing Z Data

Z is used to ramp load materials. Loading times are many 100's of ns and peak magnetic pressures are up to 2.5Mbar so propagation distances can be 100's of microns before the ramp wave steepens into a shock.

For non-dissipative materials the resulting compression wave is isentropic, providing a unique probe for the low-temperature, high-pressure region of the equation of state. Often the actual dissipation energy (from plastic work, viscosity and the like) is small compared with compression energy so that the experiments are quasi-isentropic. i.e., the deviation from isentropic compression is small and data can be treated as isentropic. The isentropic compression approach, pioneered by Barker, Asay and others, is presently being exploited by many new and innovative experimental techniques owing to the development of Z as a tool for exploring material behavior.

Early ramp loading compression experiments on copper gave a VISAR velocity history at the free surface. On a single Z experiment, such a velocity history is obtained

for more than one specimen thickness. The desire is to obtain material property data from multiple histories. VISAR velocity histories are judged by the experimenters to be accurate to 0.5ns in time and better than 1% of peak velocity.

Questions arise as to the best way to analyze the data. One way is to start with the loading history and simulate the problem, adjusting the material properties until a match with the VISAR results is obtained. This is not a satisfactory approach. The applied load, measured with Bdot probes in the Z accelerator, is inadequate for modeling purposes for two reasons. First is accuracy of the Bdot results due to calibrations and current focusing within the load. More importantly, Joule heating lowers the electrical conductivity of the specimen allowing the B-field to penetrate. Thus the acceleration experienced within the specimen arises not only from the externally applied magnetic pressure but also from both gradients in the magnetic fields that have propagated into the copper and from early-time Joule heating when inertial confinement causes pressures to rise and internal pressure gradients to form.

Before the leading disturbance reaches the free surface, the wave is simple and characteristics are straight lines. If there were no boundaries and if the same amplitude *in situ* particle velocity could be measured at two different locations, the wave speed of that amplitude of particle velocity and hence the stress-strain wound be known. Wave speed as a function of particle velocity can be related to stress-strain through the Reimann invariants. The difficulty with this approach is that *in situ* particle velocity histories must be inferred from measurement made at a free surface. As the ramp wave interacts with the free surface, reflected rarefactions propagate back into the oncoming ramp wave, lowering the stress and bending the characteristics

## Approach

These difficulties led us to try the backward integration approach. Usually in wave propagation simulations the equations of motion are solved by partitioning space and numerically stepping in time. *In this new approach, time is partitioned and the equations of motion are numerically stepped in space.* The VISAR record now becomes an initial condition and the equations are integrated back in space to the loading surface. Multiple VISAR histories should all integrate back to an identical loading history if the stress-strain material response is correct. This approach mitigates the problem of the free surface correction by properly accounting for the bending of the characteristics

The present approach has some features of Lagrangian analysis techniques pioneered by Cowperthwaite and by Fowles circa 1960-70. Forrest and Seaman applied Lagrangian analysis techniques to complex materials and Aidun and Gupta [6] present a comprehensive analysis. What is new here is addressing the case where both forward- and backward-going waves are present in the flow field. We are trying to remove free surface perturbations here rather than track the wave evolution. Also, unlike Lagrangian analysis, the present method requires choice of an analytical form material response model, although this restriction is a practical rather than a fundamental limitation as discussed later.

## Backward Method

A test problem assesses the accuracy to be expected by this technique. The following equations were used.

$$\frac{\partial \sigma_X}{\partial x} = -\rho_0 \frac{\partial u}{\partial t} \qquad \textit{momentum}$$

$$V = F(\sigma_X) \qquad \textit{material response} \qquad \textbf{(1a)}$$

$$\frac{\partial u}{\partial x} = \rho_0 \frac{\partial V}{\partial t} \qquad \textit{mass}$$

These Lagrangian equations of motion contain no convective terms because the spatial coordinates, x, move with the material.

If the motion u, at the location x is specified by an array spaced at time intervals dt, the motion can be calculated at location x+dx using second-order difference analogues for the equations of motion. Dropping the subscript x on the longitudinal stress, $\sigma_X$

$$\begin{aligned} \sigma(x+dx,t) &= \sigma(x,t) - \rho_0[(u(x,t+dt) - u(x,t-dt)]dx/2 \\ V(x+dx,t) &= F(\sigma(x+dx,t)) \\ u(x+dx,t) &= u(x,t) + \rho_0[(V(x,t+dt) - V(x,t-dt)]dx/2 \end{aligned} \qquad \textbf{(1b)}$$

The procedure is to complete step one for all times before proceeding to step two and likewise for step two before step three. These equations can be used to calculate the entire motion, stress and density fields at the new position. Repeating this entire procedure moves the solutions back yet another distance dx into the interior of the specimen, etc.

In practice, the function F(σ) is sometimes transcendental and the new volumes must be calculated from a finite differencing of the stress-strain relation. In these cases step 2 is replaced by:

$$V(x+dx,t) = V(x,t) + F'\{[\sigma(x+dx,t) + \sigma(x,t)]/2\}[\sigma(x+dx,t) - \sigma(x,t)] \qquad \textbf{(2a)}$$

More common is that the differential relating stress and volume is a function of volume rather than stress: dσ/dV=g(V). In these cases, step two is replaced by a

predictor-corrector method where V is first estimated at x+dx/2, to preserve the second order accuracy of the equation set:

$$V_H = V(x,t) + \{\sigma(x+dx,t) - \sigma(x,t)\} / 2g'(V(x,t))$$
$$V(x+dx,t) = V(x,t) + [\sigma(x+dx,t) - \sigma(x,t)] / g'(V_H) \quad \textbf{(2b)}$$

## Boundary Conditions on Time

Care must be taken to ensure that the time domain is initially selected large enough to accommodate the solution. For instance, if the first motion of the VISAR record is at time $t = t_0$, first motion at depth X from the VISAR measurement surface will occur at $t = t_0 - X/C_0$. Therefore, the VISAR time array must begin at or before this time. Similarly, if the last valid VISAR measurement occurs at $t = t_1$, the backward solution will only be valid at times less than how far back in time the left-going characteristic from x=0, $t= t_1$ can propagate. Restricting solutions to inside of these "world lines" ensures the time boundary conditions do not influence solutions.

## Testing the Backward Method

To test the method we began with a traditional forward solution to an initial-value problem using WONDY, a well-known finite difference code [7]. A 0.491mm slab of copper, initially at rest was subjected to the Z-452 ramp pressure load on the left-hand boundary. V(p) was chosen as the known principal isentrope for copper. The result of this traditional calculation was a simulated VISAR history at the rear surface of the copper that could be used as an "initial condition" for our backward test. The "backward" difference equations described above were integrated in space from x = 0.491mm back to the original loading surface at x = 0. A comparison of the starting profile with the backward-regenerated profile in Figure2 shows the method accurate to about ± 0.3ns or about ± 0.5kbar.No effort has been made to improve this accuracy of this particular calculation but it is likely that it could easily be done. With sufficiently fine zoning, there appears to be no practical limit to the achievable accuracy for idealized problems like this.

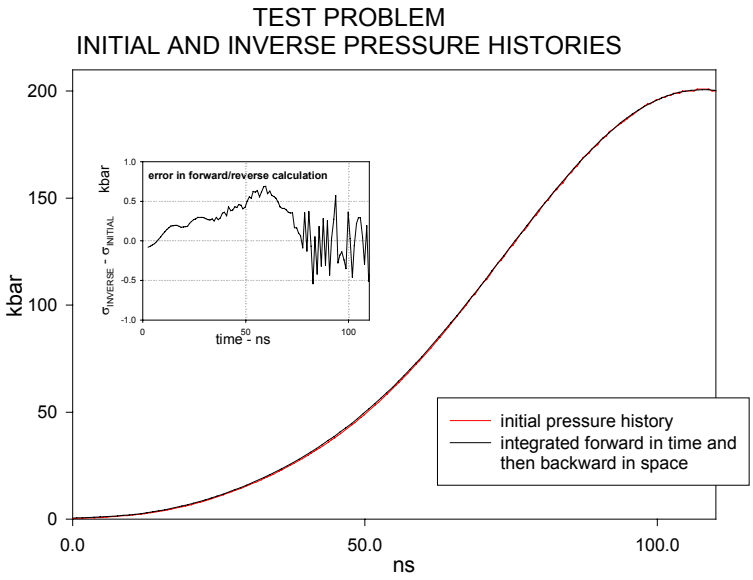


**Figure 2**. The initial pressure history was used as a boundary condition in the WONDY code. It was applied at x=0 to a copper specimen to calculate a simulated VISAR record at x=0.491mm. This simulated VISAR record was used as an initial condition and the equation of motion were integrated backward in space to x=0. The pressure history re-generated with the backward method agrees with the initial pressure history to better than ¼%. No attempt was made to refine the calculation. There appears to be no practical limit to the accuracy of the backward calculation for an idealized problem like this; refining the time-space mesh will produce even better agreement.

## Applying the Method to Z Data

Z-452 was actually an early Z experiment with experimental VISAR histories for copper samples of 0.491 and 0.808mm thickness. See Figure 3. We applied the backward method to those Z-452 experimental results. The relation we are seeking is $V(\sigma_X)$. Backward calculations were made with a Murnaghan form.

$$B_S(V) = B_{S0}\left(\frac{V_0}{V}\right)^{B'} \qquad \textbf{(3)}$$

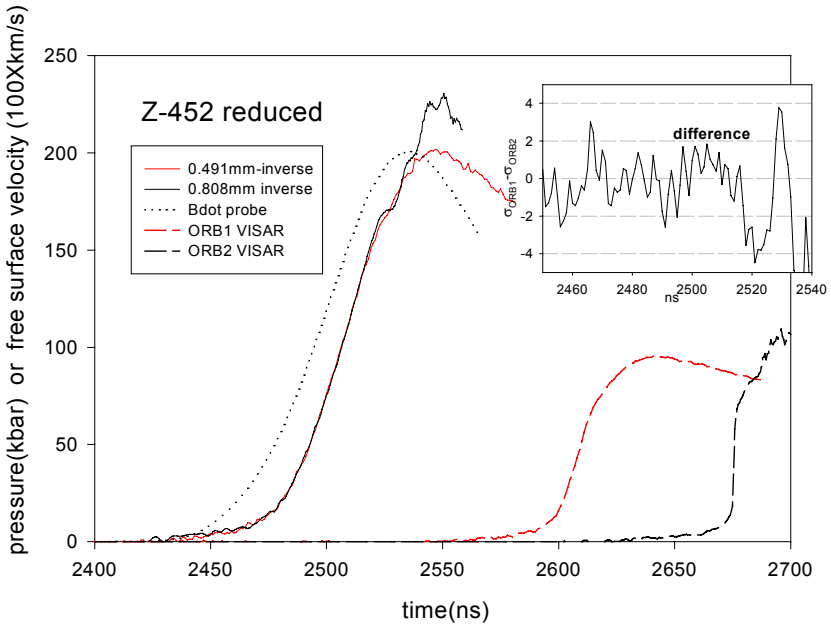


**Figure 3.** Two VISAR records from copper samples of two different thicknesses were obtained during a single Z experiment. Each free surface record was integrated backward in space to x=0. The stress-strain relation was varied systematically until the two calculated load histories at x=0 were the same. They agree to about 1%. The deduced stress-strain agrees with the known behavior of copper and is shown in a later figure.

Each VISAR record was integrated back to x=0 and the two inferred pressure histories compared. On the first attempt, they do not agree. The Murnaghan parameters $B_{S0}$ and $B_S'$ were varied repeatedly in a systematic way and the equations integrated backward in space to find the parameter values that gave the best agreement between the two pressure load histories. Those are:

| | $B_{So}$ (Mbar) | $B_S'$ |
|---|---|---|
| Z-452 | 1.4861 | 4.1911 |
| Z-516 | 1.3493 | 4.8567 |

For Z-452, the difference in time at fixed particle pressure between two calculated initial load histories (Figure 2) is about 1ns with most of the difference coming from noise in the original VISAR records. There is little systematic difference.

The entire procedure was repeated for a different experiment, Z-516. Z-516 is qualitatively similar showing good agreement for most of the inferred compression history at the front surface. Figure 4 overlays the two inferred loading profiles. Between 20 and 180 kbar, RMS timing differences over the relevant pressure interval are about 0.3ns. The loading profile from the Bdot probe is also shown for Z-452. Bdot loading occurs about 10ns too early to match our analysis. The difficulty of field penetration discussed earlier should lead to a Bdot record that is later in time and not leading the inverted VISAR records in time as is seen. This anomaly is not resolved here but the calculation is more likely correct.

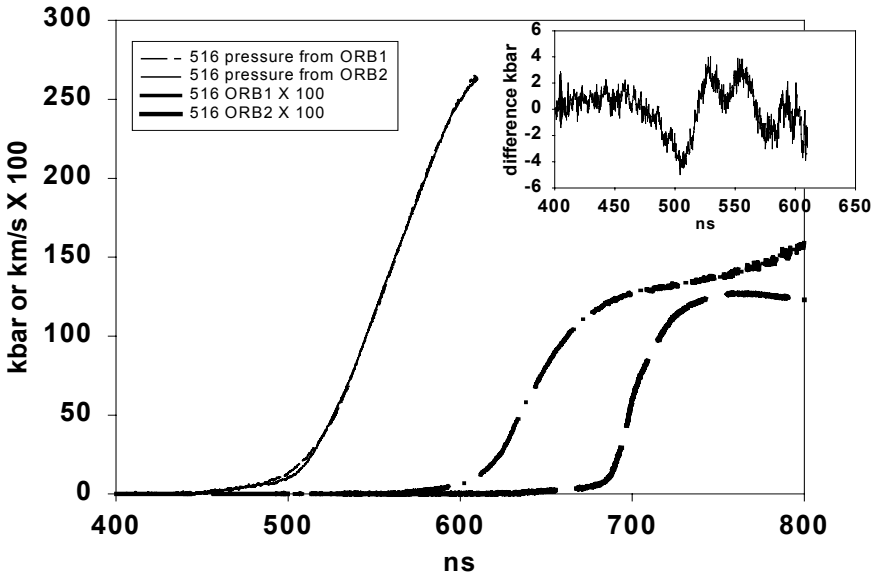


**Figure 4.** Analysis of Z-516. The caption of Figure 3 pertains to this figure as well.

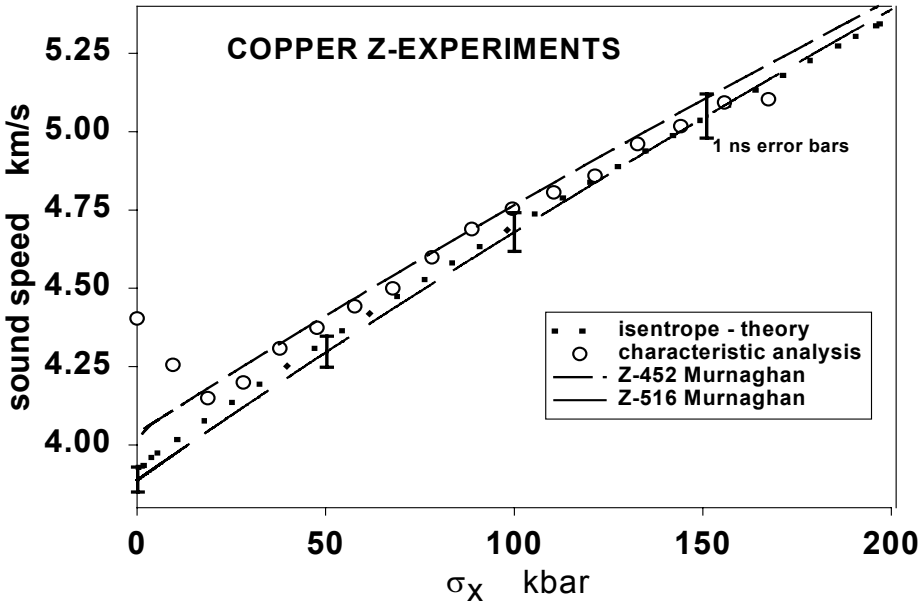


**Figure 5.**The stress-strain relation (shown as sound speed versus stress) for copper deduced from the backward method compared with the known behavior of copper.

$$C^2 = -V^2 \frac{\partial p}{\partial V}\Big)_S$$

Figure 5 shows Lagrangian bulk sound speed as a function of longitudinal stress for the best fit and is compared with results using the characteristic method described

earlier. The theoretical isentropic Lagrangian bulk sound speed for pure copper is also shown for comparison.

## Discussion

Several points are noteworthy. Clint Hall [8], the Sandian who performed these experiments has applied a traditional characteristics analysis to Z-452. Our best-fit analysis using backward integration compares favorably with that analysis. The slightly stiffer best fit probably derives from our more accurate free surface treatment. Time differences of about 1ns are sufficient to account for the difference in best-fit and traditional results (Figure 5). These experiments had peak stress of about 200kbar. Differences between backward solutions and characteristic solutions are much larger in experiments above 1Mbar that are presently being analyzed.

Both the traditional and the backward analysis technique give sound speeds for Z-452 that are larger than for a pure copper result. Some of this may stem from the experiments measuring longitudinal stress, not pressure and because the yield strength in copper is known to increase with plastic strain in some alloys of copper.

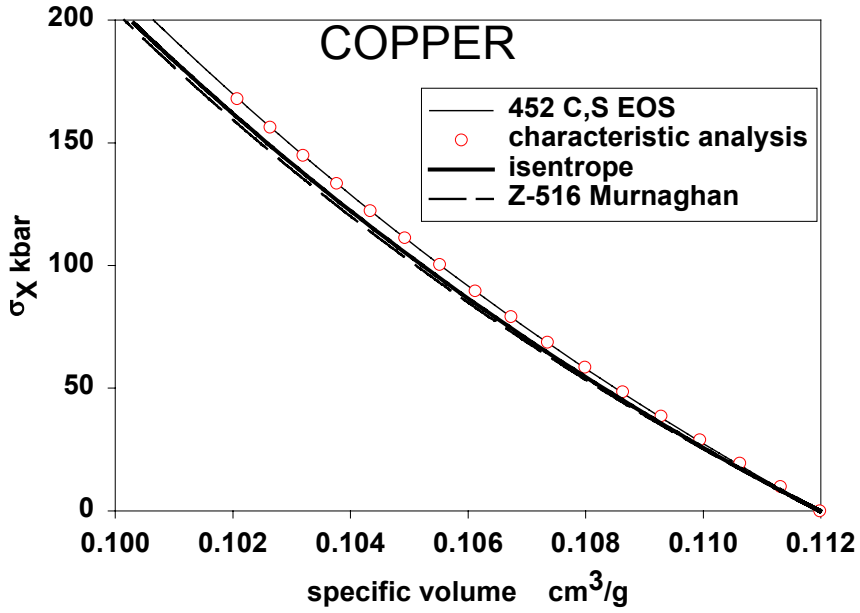


**Figure 6.** The deduced stress-strain behavior of copper compared with the known behavior. For experiment 516, the two curves lie on one another and cannot be seen as separate in the above diagram.

## Other Than Free Surfaces

There is no reason to restrict application of this method to free surface VISAR histories. Whenever the stress-strain relationship is known for the window, one need only

initialize the boundary conditions appropriately. For a VISAR window like LiF in a copper experiment, the initial histories are configured:

| | |
|---|---|
| Particle velocity - u(t) | LiF window velocity from VISAR |
| Stress - $\sigma_X(t)$ | LiF window stress at this u(t) |
| Volume – V(t) | Copper volume at this stress |

Having initialized the backward problem in this way, no other account of the window need be made; the problem is integrated back into the copper as usual. Note, however, that the problem is implicit in that the stress-strain "answer" is required to initialize the integration. While this leads to larger uncertainties in the stress-strain result, the method is robust for two-specimen problems and satisfactory convergence is always achieved.

We performed a check on this method. David Reisman [9], used the TRACII code to simulate VISAR histories for two different thicknesses of copper, each backed by LiF windows. We performed the backward analysis on these VISAR histories and deduced both the loading history and the stress-strain relation for the copper. Comparison of the starting and deduced stress-strain relationship is shown in Figures 7. The agreement is remarkably good considering that we each used our own, slightly different description for the σ-u isentrope of LiF. Figure 8

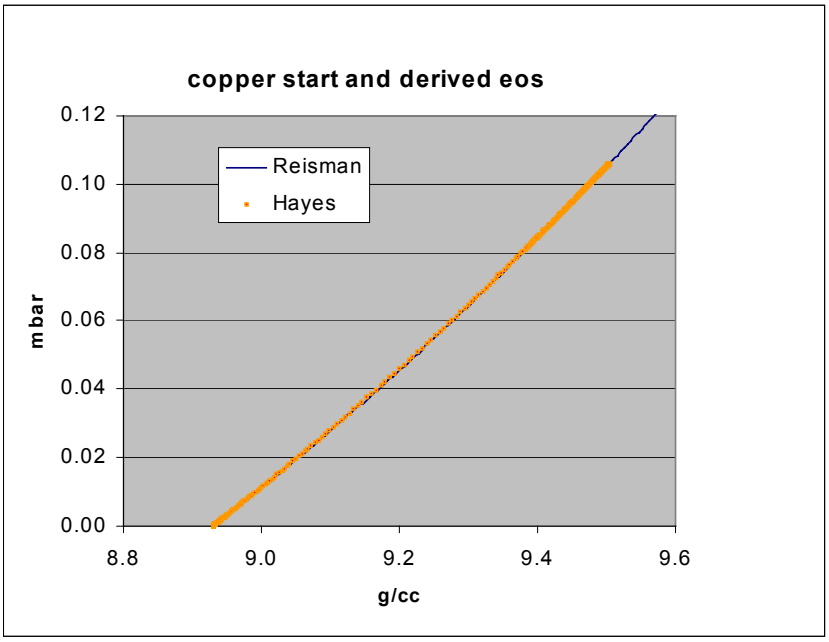


**Figure 7.** Backward was used to analyze a pair of simulated VISAR records. The load was applied to two different thicknesses of copper. Each copper slab was backed by a LiF window and the predicted VISAR histories were generated. The stress-density behavior of copper was deduced by the backward calculation directly from these simulated VISAR histories and compares well with the one actually used by Reisman.

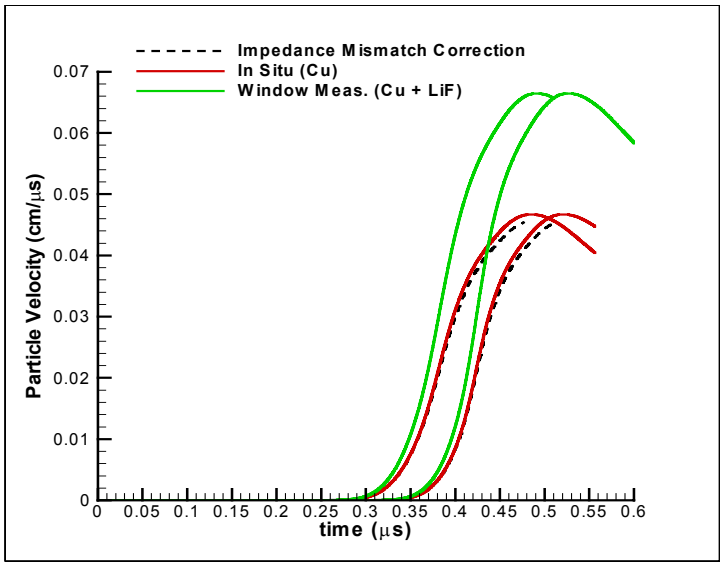


**Figure 8.** Reisman's two simulated VISAR records that were used in the backward calculation. The method of Grady and Young, used to estimate what the *in situ* particle velocity would have been if no interface were present, is compared with TRAC II results of calculated *in situ* velocities. Errors are as large as about 10ns by using this procedure Backward integration deduced the load history in a rather exact way (see Figure 9), so calculating the *in situ* velocities by backward integration of the VISAR records followed by forward integration of the problem in TRAC II gives a precise result of the *in situ* results (not shown). For this idealized example the backward method makes essentially an exact correction for the window interface perturbations.

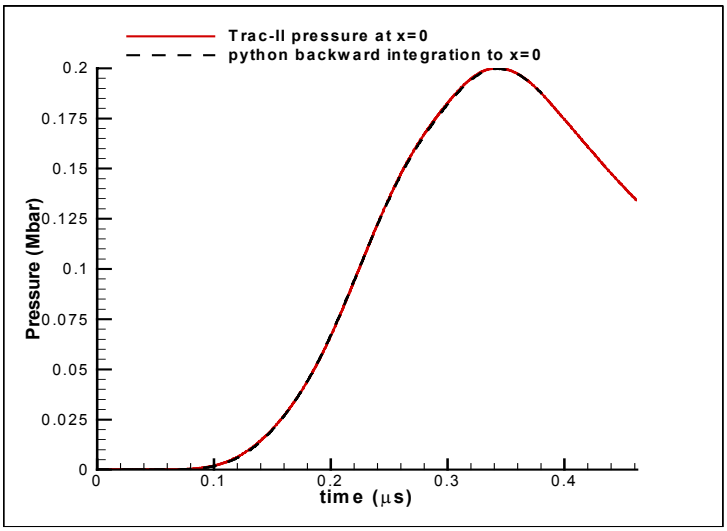


**Figure 9.** Reisman's load history compared with that deduced from backward integration of the VISAR records. They agree almost exactly.

shows the starting simulated VISAR records, the calculated *in situ* records and an attempt to infer the second from the first using one of the approximate methods. Agreement is not good. On the other hand, backward *in situ* calculations are essentially exact. Figure 9 shows the deduced load agrees almost exactly with Reisman's starting load.

## Elastic-Plastic (E-P) Material

It is possible to treat materials that have hysteretic stress-strain relations. Above, we did not distinguish between longitudinal stress and pressure. This distinction is necessary for treating elastic-plastic materials. Define terms as follows:

$\sigma_X$ – longitudinal stress (below, when the subscript x is omitted, $\sigma_x$ is implied).
P – pressure
$\tau$ – shear stress = $(\sigma_X-\sigma_Y)/2$
x – Lagrangian position
$\nu$ – Poisson's ratio
Y – yield strength
$\varepsilon$ – volumetric strain
$\varepsilon = E(P)$ – function relating volumetric strain and hydrostatic pressure

In the backward numerical method described above, momentum conservation, equation of state and mass conservation were solved in that order. For E-P treatment, steps 1 and 3 remain the same and only the equation of state is treated differently, being supplemented by the elastic-plastic constitutive relation. The time integration of the elastic-plastic relations at the new position x proceeds as follows:

$$\tau(x, t+dt) = \tau(x,t) + \frac{1-2\nu}{1-\nu}(\sigma(x,t+dt) - \sigma(x,t))/2 \quad \textbf{(4)}$$

*subject to*

$$\left|\tau(x,t+dt)\right| \le \frac{Y}{2} \quad \textbf{(5)}$$

The latter equation is the von-Misis yield condition. If the inequality is not met, the shear stress is set on the upper or lower yield surface as appropriate:

$$\tau(x,t+dt) = \pm\frac{Y}{2} \quad \textbf{(6)}$$

The new strain is then easily calculated

$$\varepsilon(x,t+dt)=E[\sigma(x,t+dt)-4/3\tau(x,t+dt)] \quad \textbf{(7)}$$

As before, sometimes E is transcendental and a predictor/corrector method is required to calculate the new strain to second order accuracy

# Comments on the Method

## General Considerations

There are few limitations on the complexity that could be introduced in material models although in practice the method can be very computationally intensive. Two free parameters (n=2) were optimized in 10's of minutes on a 450MHz. We have recently implemented the Amoeba minimization method from **Numerical Recipes** by Press and early examples show considerable speedup when n is greater than 3. This has allowed our stress-strain relation to be expressed, for instance, through Lagrangian sound speed being a quartic polynomial in pressure. This has been used recently to analyze a Z experiment in aluminum to 1.1Mbar. The analysis is not shown here.

Integration can be done backward in space to any convenient location, provided it is far enough back to avoid perturbations from the free surface at earlier times of interest. The same stress-strain behavior would be obtained in the copper experiment on Z if the integration were carried back to say 0.1mm, 0mm as was done above, or even to –0.1mm! The position x=0 is usually chosen although the inferred loading profile at the 0mm location is not the one actually experienced by the copper whenever the magnetic field has penetrated the copper during loading. In that case, the experimental ramp load is applied to the copper in depth through a combination of magnetic pressure and because of gradients in the magnetic field in the specimen, which couple through the momentum conservation equation. It is likely that such skin depth effects are small in the present case and that the inferred loading history reasonably reflects the actual magnetic pressure history. However, the important results obtained with the backward method are unaffected by this uncertainty.

As long as the stress-strain relation is unique, no shocks appear in the solutions and the time boundary conditions do not penetrate the solution, the governing equations are hyperbolic and there are no practical limitations to the number of layers of different materials or the number of reverberations that can be accommodated in a backward solution.

For situations where E(p) is known, it would probably be easier to integrate Eqs. (1a) using a commercial PDE solver. However, E(p) is often transcendental and the introduction of strength into material models makes the equations parabolic. Therefore, it is more convenient to use our own numerical procedure.

A general question arises about the numerical stability of these equations. Without strength effects, the entire equation set is hyperbolic and presumably one can numerically integrate backward and forward in time or space with impunity. We usually select $dx < C_L dt$ for this situation. But by adding strength, the equations become parabolic in time.

The fundamental stability of numerical solutions to these equations has not yet been determined. In *lieu* of analyzing the stability limit for space steps appropriate to this equation set [for parabolic equations, $dx \sim (dt)^{1/2}$], we simply decreased the space step until satisfactory results were consistently achieved. This was about 5% of the equivalent "Courant condition" –the Courant condition prevents disturbance speed from exceeding mesh speed.

Sometimes our elastic-plastic solutions develop instabilities. In those cases, stress and particle velocity are lightly smoothed every 25 space steps to suppress these. e.g.,

$$u(x,t) \leftarrow u(x,t)/2 + [u(x,t+dt) + u(x,t-dt)]/4 \qquad \textbf{(8)}$$

We have determined that smoothing every 10-50 space steps has no influence on the ultimate solution for most problems. Smoothing well outside these frequency bounds leads to unacceptable errors in the solution.

When a backward-determined stress history at some interior location is used in a subsequent forward calculation, the starting simulated VISAR history is **always replicated, even if the material model is incorrect***,* provided the integrations were done accurately. Because the same equations are being integrated back in space and then forward in time, backward integration can proceed to essentially any location in the interior of the specimen, the stress history at that location used in WONDY for a forward calculation, and the original VISAR record recovered. That is why another constraint must be found to make use of this method. For Z experiments, this constraint is usually that two specimen thicknesses must both produce the same load. This constrains the specimen stress-strain relation. For determining gradients in an accelerating flyer plate, which is shown in a subsequent example, the stress-strain relation must be known. For the spall experiment that is given as another later example, stress after spallation must remain zero at the spall plane, etc.

## Additional Examples

The backward integration method is presently being used to analyze a variety of experiments at Sandia, Los Alamos and Lawrence Livermore National Labs. Below are two more that show the breadth of application.

Starting from a free surface velocity history from a spall pullback experiment in aluminum (John Vorthman, LANL) [10], determine the location of the spall plane and the stress history of the failure process at that location. Also determine parameters for the time-dependent quasielastic model of plasticity. (Figure 10)

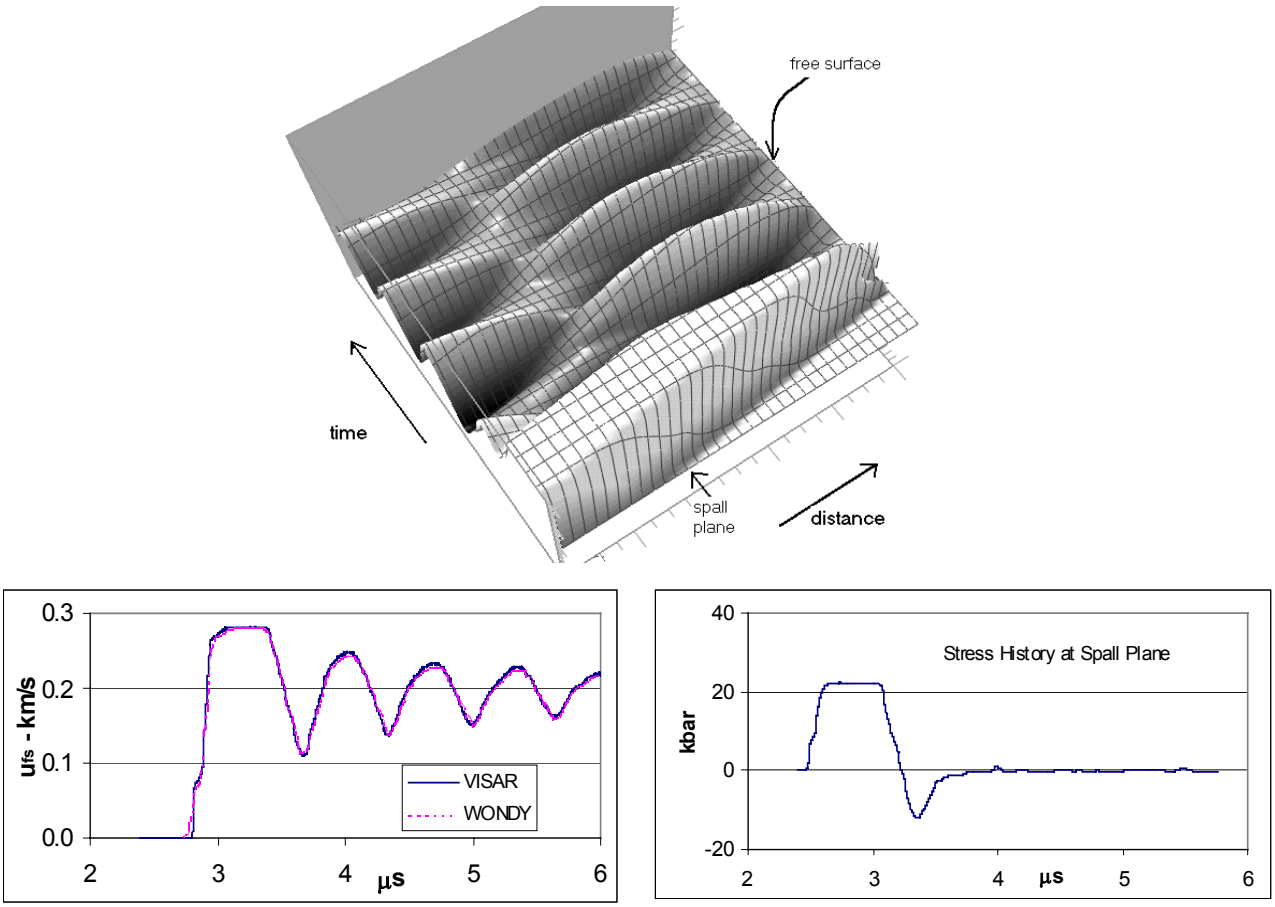


**Figure 10.** Results from backward integration of a spall pullback free surface VISAR experiment on 6061-T6 aluminum. The VISAR free surface record (lower left) was integrated backward in space to ~150% of the estimate scab thickness. The 3-D graph shows the calculated stress as function of time and Lagrangian distance from the free surface. Note the slice marked "spall plane". That is the plane where the stress stays at zero after spall occurs. Stress at that plane is also shown in the lower right graph. The backward integration sought best values for the two quasielastic parameters and for the position where the RMS of the late time stress was a minimum. Two quasielastic parameters deduced for 6061-T6 Al agree well with those determined by Johnson. The position of the deduced spall plane agrees with experiment. The two-step failure seen in the lower right graph displays secondary spall resistance behavior seen previously in tantalum. The calculated free surface velocity (lower left) was obtained with WONDY where the backward-determined load (lower right) was applied to an aluminum layer with thickness equal to the backward-determined scab thickness [5]. The VISAR record and the WONDY simulation agree almost exactly.

Starting from a 13km/s shockless flyer plate acceleration (Marcus Knudson) [11], determine density, stress and particle velocity gradients in the flyer at impact time. (Figure 11)

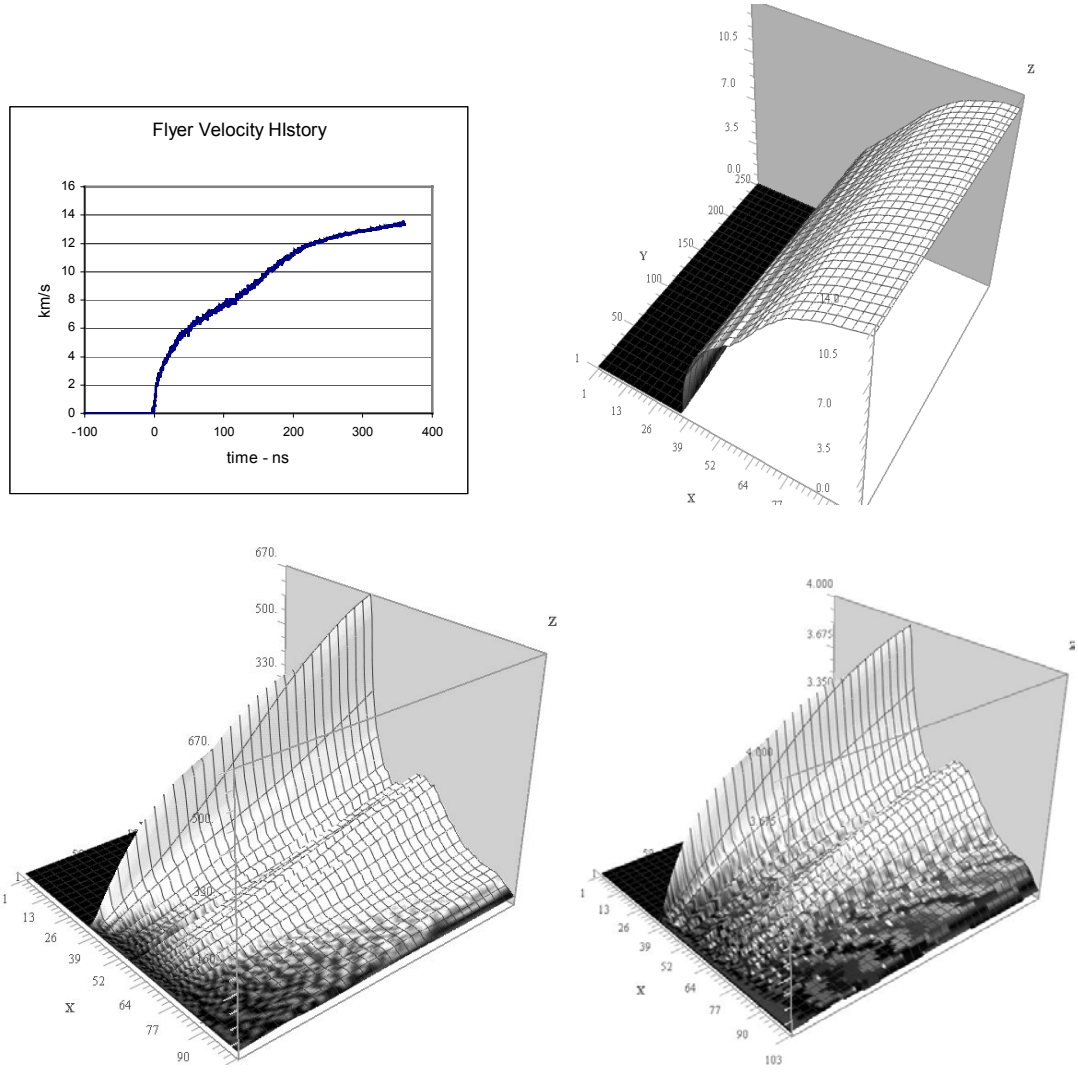


**Figure 11.** Analysis of a high velocity flyer plate. The VISAR-measured velocity (upper left) was used in conjunction with the backward method to determine gradients in the flyer at impact time. In the remaining three figures, x is time and y is Lagrangian depth from the free surface. Upper right is particle velocity; lower left is pressure and lower right density. Impact time is approximately 350ns which is approximately x = 90 in these 3-dimensional graphs. The measured particle velocity can be seen as the Y=1 slice in the upper right. The experimenter (Marcus Knudsen, SNL) used gradients in density, pressure and particle velocity at impact time as initial conditions at this time for a subsequent WONDY calculation to estimate the effects of gradients in the flyer plate on the shock induced in the target (target not shown).

Each of these examples is part of an ongoing experimental study in which the backward method is finding application.

# Conclusion

There are many combinations of forward/backward analyses that can be used to interpret experimental data. For instance, if one specimen of a two-specimen Z experiment has a shock, the shockless result can be integrated backward and the specimen with a shock integrated forward with a code like WONDY. By demanding the calculated and measured shock results agree, the equation of state could be determined. Or if a window has an unknown stress-strain relation but the sample is calibrated, two experiments could define that unknown. Recent experiments by Clint Hall [8] have combined free surface and window measurements in a unique way to define window optical properties. The backward method is an essential part of this investigation. There is seemingly an endless variety of ways to put forward and backward calculations together to tease new results from experiments, provided we can shed our habit of viewing the x-t plane from only one direction.

# References


1. L. Barker and R. Hollenbach, Journal of Applied Physic, **43**, 4669, 1972.

2. D. Reisman, et.al., Journal of Applied Physics, **80**, p. 1625, 2001.

3. D. Grady and E. Young, "Evaluating Constitutive Properties From Velocity Interferometer Data", Sandia National Laboratories Report, SAND75-0650, 1975.

4. J. N. Johnson, J. Phys. Chem. Solids **54** (6) pp. 691-699, 1993.

5. D. Hayes, J. Vorthman and J. Fritz, "Backward Integration of a Spall VISAR Record to the Spall Plane", DX-1, Los Alamos National Laboratory, LA-13830-MS, June 2001.

6. J. Aidun and Y. Gupta, Journal of Applied Physics, **69**, p. 6998, 1991.

7. M. Kipp and R. Lawrence, "WONDY-V – A One Dimensional Finite Difference Wave Propagation Code", Sandia National Laboratories Report, SAND81-0939, 1982.

8. Private Communication, Clint Hall, Sandia National Laboratories.

9. Private Communication, David Reisman, Lawrence Livermore National Laboratory.

10. Private Communication, John Vorthman, Los Alamos National Laboratory.

11. Private Communication, Marcus Knudson, Sandia National Laboratories.

# Distribution

## EXTERNAL DISTRIBUTION:

Los Alamos National Laboratory
Mail Station 5000
P.O. Box 1663
Los Alamos, New Mexico 87545

Attn: Bill Anderson MS P952 DX-1
Attn: Joe Fritz MS P952 DX-1
Attn: George Gray III MS P952 DX-1
Attn: Allan Hauer MS E527 NW-EP
Attn: Dennis Hayes MS P952 DX-1
Attn: Rob Hixson MS P952 DX-1
Attn: David Holtkamp MS D410 P-22
Attn: Yuki Horie MS D413 X-7
Attn: Ralph Menikoff MS B214 T-14
Attn: Dennis Paisley MS E526 P-24
Attn: Alan Picklesimer MS F613 NW-EP
Attn: Steve Sheffield MS P952 DX-1
Attn: Davis Tonks MS D413 X-7
Attn: John Vorthman MS P952 DX-1

Lawrence Livermore National Laboratory
7000 East Avenue
Livermore, California 94550

Attn: Bob Cauble MS L-041
Attn: Elaine Chandler MS L-097
Attn: Mike Dunning MS L-097
Attn: Jerry Forbes MS L-282
Attn: Lee Griffith MS L-125
Attn: Neil Holmes MS L-045
Attn: Warren Hsing MS L-021
Attn: David Reisman MS L-041
Attn: Bruce Remington MS L-021

Dennis Grady
Applied Research Association, Inc.,
4300 San Mateo NE, Suite A220
Albuquerque, New Mexico 87110

Nancy Winfree
9813 Admiral Dewey Ave. NE
Albuquerque, New Mexico 87111

AWE
Aldermaston, Reading
Berks RG7 4PR,
England

Attn: Mike Dunne
Attn: Kenneth Parker
Attn: James Palmer
Attn: Steve Rothman,

Rod Clifton
Brown University
182 Hope St.,
Providence, Rhode Island 02912

Caltech
1200 East California Blvd.
Pasadena, California 91125

Attn: Tom Ahrens MS 252-21
Attn: Joe Akins MS 252-21

Gerry Kerley
Kerley Publishing Services
P.O. Box 13835
Albuquerque, New Mexico 87192-3835

John Remo
Quantametrics Inc.,
#1 Brackenwood Path,
Head of the Harbor
St. James, New York 11780

Don Curran
723 Canyon Road
Redwood City CA 94062

Jim Johnson
7201 Stanich Ave. NW
Gig Harbor, WA 98335

Larry Lee
Ktech Corporation
2201 Buena Vista SE, Suite 400
Albuquerque, New Mexico 87106

Andrew Ng
University of British Columbia
Dept. of Physics & Astronomy
6224 Agricultural Rd.
Vancouver, BC V6T 1Z1, Canada

Jow Ding
Washington State University, Institution of Shock Physics
P.O. Box 642816
Pullman, Washington 99164-2816

Yogi Gupta
P.O. Box 642816
Pullman, Washington 99164-2816

Paul Drake
Atmospheric, Oceanic & Space Sciences

Space Physics Research Laboratory
2455 Hayward St.,
University of Michigan
Ann Arbor, Michigan 48109-2143

## SANDIA INTERNAL:

| | |
|---|---|
| MS 0310 | Paul Yarrington |
| MS 0316 | John Aidun |
| MS 0318 | Mark Boslough |
| MS 0819 | Tim Trucano |
| MS 0820 | Pat Chavez |
| MS 0820 | David Crawford |
| MS 0820 | Paul Taylor |
| MS 0824 | Art Ratzel |
| MS 0834 | Wayne Trott |
| MS 0836 | Mel Baer |
| MS 0836 | Gene Hertel |
| MS-0836 | Robert Schmitt |
| MS 0847 | Hal Morgan |
| MS 1159 | Bill Barrett |
| MS 1159 | Mark Hedemann |
| MS 1168 | Tom Bergstresser |
| MS 1168 | Chris Deeney |
| MS 1168 | Mike Furnish |
| MS 1178 | Doug Bloomquist |
| MS 1179 | Jim Lee |
| MS 1181 | Jim Asay |
| MS 1181 | Lalit Chhabildas |
| MS 1181 | Jean-Paul Davis |
| MS 1181 | Clint Hall |
| MS 1181 | Dennis Hayes (25) |
| MS 1181 | Marcus Knudson |
| MS 1181 | Bill Reinhart |
| MS 1186 | Ray Lemke |
| MS 1186 | Tom Mehlhorn |
| MS 1191 | Keith Matzen |
| MS 1194 | Dillon McDaniel |
| MS 1391 | Dave Thomson |
| MS 1411 | Eliot Fang, 1800 |
| MS 1421 | Mark Anderson |
| MS 1421 | George Samara |
| MS 1421 | Bob Setchell |
| MS 1454 | Lloyd Bonzon |
| MS 1454 | Anita Renlund |
| MS 9401 | Craig Henderson |
| MS 9402 | Ken Wilson |
| MS 1674 | Mike Desjarlais |
| MS 9405 | Rick Stulen |
| MS 9161 | Er-Ping Chen |
| MS 9018 | Central Technical Files, 8945-1 (1) |
| MS 0899 | Technical Library, 9616 (2) |
| MS 0612 | Review and Approval Desk, 9612 For DOE/OSTI (1) |